Journal of The Korean Astronomical Society
37: 605 ∼ 609, 2004

3D SIMULATIONS OF RADIO GALAXY EVOLUTION IN CLUSTER MEDIA

Sean M. O'Neill[1], Paul Shearer[1], Ian L. Tregillis[2], Thomas W. Jones[1], and Dongsu Ryu[3]
[1] Department of Astronomy, University of Minnesota, 116 Church Street SE, Minneapolis, MN 55455, USA
[2] Applied Physics Division, MS B259, Los Alamos National Laboratory, Los Alamos, NM 87545, USA
[3] Department of Astronomy & Space Science, Chungnam National University, Daejon 305-764, Korea
E-mail: smoneil@msi.umn.edu, shearerp@msi.umn.edu, twj@msi.umn.edu, iant@lanl.gov, ryu@canopus.chungnam.ac.kr

ABSTRACT

We present a set of high-resolution 3D MHD simulations exploring the evolution of light, supersonic jets in cluster environments. We model sets of high- and low-Mach jets entering both uniform surroundings and King-type atmospheres and propagating distances more than 100 times the initial jet radius. Through complimentary analyses of synthetic observations and energy flow, we explore the detailed interactions between these jets and their environments. We find that jet cocoon morphology is strongly influenced by the structure of the ambient medium. Jets moving into uniform atmospheres have more pronounced backflow than their non-uniform counterparts, and this difference is clearly reflected by morphological differences in the synthetic observations. Additionally, synthetic observations illustrate differences in the appearances of terminal hotspots and the x-ray and radio correlations between the high- and low-Mach runs. Exploration of energy flow in these systems illustrates the general conversion of kinetic to thermal and magnetic energy in all of our simulations. Specifically, we examine conversion of energy type and the spatial transport of energy to the ambient medium. Determination of the evolution of the energy distribution in these objects will enhance our understanding of the role of AGN feedback in cluster environments.

Key words : galaxies: jets – methods: numerical – MHD – radiation mechanisms: nonthermal

I. INTRODUCTION

The basic model of radio galaxies as jet-driven systems is now well-established, but the specific nature of radio jet interactions with the ambient medium remains largely unexplored. Radio jets are commonly invoked as the mechanisms potentially responsible for a seemingly disparate set of astrophysical phenomena, including the re-introduction of energy into galaxy cluster environments (e.g. Blanton *et al.* 2003, Böhringer *et al.* 2002, Churazov *et al.* 2002). With an efficient means by which to solve both the large-scale dynamics and nonthermal particle transport, we can now begin to address very specific questions about the role of environment in the evolution of radio galaxies, including the influence of the structure of ambient atmospheres on jet propagation and the contribution of jet Mach number to the overall morphology and behavior of the system.

II. SIMULATIONS

(a) Numerical Methods

Our simulations employ a second-order conservative total variation diminishing (TVD) ideal MHD code based on that of Harten (1983), as described in Ryu & Jones (1995) and Ryu *et al.* (1995). The code maintains a divergence-free magnetic field at each time step using a constrained transport scheme (Dai and Woodward (1998); Ryu *et al.* (1998)). A gamma-law gas equation of state is assumed with $\gamma = 5/3$. Additionally, a passive mass fraction, or "color" tracer is introduced at the jet orifice to track jet material as it propagates through the computational grid.

Nonthermal electron transport is followed through solution of the standard "convection diffusion" equation for the particle momentum distribution including diffusive shock acceleration, plus radiative and adiabatic losses, as detailed in Jones *et al.* (1999) and Tregillis *et al.* (2001). The momentum distribution of nonthermal particles relevant to radio synchrotron and x-ray inverse Compton emission is sufficiently broad that our transport scheme represents it as a piecewise power-law across a few broad bins in momentum space and integrates the convection diffusion equation across these coarse bins. Furthermore, the mismatch between the characteristic bulk flow lengths and timescales and the scales relevant to electron diffusive acceleration and transport allows us to treat shock acceleration of relevant nonthermal particles as an instantaneous process, providing a computationally efficient means for calculating the electron momentum distributions. Tracking nonthermal particles in this way allows us to construct synthetic observations from our data in a self-consistent fashion.

Proceedings of The 3rd Korean Astrophysics Workshop on
Cosmic Rays and Magnetic Fields in Large Scale Structure

(b) Global Simulation Parameters

Here we detail the general properties of the four simulations, followed by a description of those properties specific to each run.

Our simulated jets entered from the midpoint of the $x = 0$ plane. All four simulations followed jet propagation to lengths approximately 115 initial jet radii, or 230 kpc in the x direction. The grid was uniform in x with $\Delta x \approx 0.4$ kpc. In order to keep the entire bow wave structure produced by the jet within the computational domain, a nonuniform grid was applied in the y and z directions. Distances within 25 kpc of the jet origin in those two coordinates were resolved on the same uniform grid as in the x coordinate. Beyond that, the computational zones in those two directions expanded logarithmically. The full extent of the computational domain in y and z varied with the simulation, depending on its duration, but was in each case at least 230 kpc.

Apart from the inflow through the jet orifice in the $x = 0$ plane, the four simulations described employed open boundary conditions everywhere. Since the initial conditions are never disturbed on any other than the $x = 0$ plane, only that one choice really has any consequence. Our choice of open boundaries there reflects our interpretation of the inflow region as being located downstream from the true jet origin and collimation region, so away from any reflection symmetry. To evaluate the significance of this choice of boundary conditions we carried out two different tests. First, we computed the total energy leaving the grid through the $x = 0$ plane as a result of jet backflow and disturbed ICM. As discussed below the escaped energy was generally less than about 10% of the energy brought onto the grid by the jet during its life. That should be too small to have any major impact. To test this we also conducted a comparison run identical to the model HU described below, except that we assumed in that case reflecting boundaries outside the jet orifice in the $x = 0$ plane. Although there were modest differences in the detailed properties of the two simluations, they were qualitatively similar, and the conclusions relevant to this study would be the same from either simulation.

(c) Ambient Medium

We explored two simple models for the ICM confining the jets; namely uniform (designated 'U' below) and plane stratified media. The stratified ICM was a simple, isothermal King model (King 1962) (designated 'K' below) of the form

$$\rho_a(x) = \frac{\rho_0}{(1 + (\frac{x}{x_c})^2)} \tag{1}$$

where ρ_0 is the density at $x = 0$ and x_c is the core "radius" of the atmosphere, chosen to be 1/3 of the total grid length. Since the ICM is isothermal the pressure distribution is simply $P(x) = c_a^2 \rho(x)/\gamma$, where c_a is the ICM sound speed, chosen according to jet Mach number as discussed below. The initial condition of hydrostatic equilibrium then determines the form of the gravitational acceleration in the King atmosphere to be:

$$g(x) = -\frac{2c_a^2}{\gamma} \frac{x}{x_c^2 + x^2} \tag{2}$$

The structure of the ambient magnetic field was identical for each of the four simulations. The initial ambient field consisted entirely of a uniform poloidal component (B_{x0}) that exerted a magnetic pressure 1% of the initial ambient gas pressure ($\beta = P_g/P_B = 100$) at the base of the grid.

(d) Jet Properties

The jets entered the computational grid with a top-hat velocity profile of $v_j = 0.15c$ in the jet core, which had a radius of 2 kpc. The jets were in approximate pressure equilibrium with the ICM and featured a density contrast of $\eta = \rho_{jet}/\rho_{amb} = 10^{-2}$ as they entered. The resulting ambient sound speed is used as a unit speed, while the jet radius provides a convenient length scale. The associated computational time unit becomes $r_j/c_a = 1$. To develop a fully 3D flow as early as possible in each simulation, jet axisymmetry was explicitly broken through a slow jet "wobble" introduced in the inflow region. In each case, the jet swept out a cone of opening angle 3 degrees over a time scale several times shorter than the simulation time.

To explore the importance of jet Mach number in determining dynamical and radiative properties we simulated jets in each of the ICM atmospheres mentioned earlier with jet orifice internal Mach numbers $M_j = 12$ (external Mach number, $M = v_j/c_a = 120$) and $M_j = 3$ ($M = 30$). We designate the high Mach number, $M_j = 12$ simulations by the letter 'H', and the low Mach number, $M_j = 3$ runs by 'L'. Thus, the four models discussed are labelled HU and LU in the uniform medium and HK and LK in the stratified, King atmosphere. The jet kinetic luminosities are given by $L_k \approx (1.1 \times 10^{44}) M_j^2$ erg s^{-1}, and propagation times across the grid ranged from roughly 40 Myr in the King atmosphere to about 65 Myr in the uniform medium.

The jet magnetic field consists of toroidal and poloidal components. Its magnitude was chosen to be roughly representative of magnetic fields in real radio galaxies. The poloidal field was identical to that of the ambient medium, while the toroidal field was of the form $B_{\phi 0} = 2 \times B_{x0}(r/r_j)$ for $r \leq r_j$, where $B_{\phi 0} = 6$ μG at the edge of the jet core. The region surrounding the jet core contained a six-zone buffer in which the velocity and magnetic field were smoothly decreased to their ambient values.

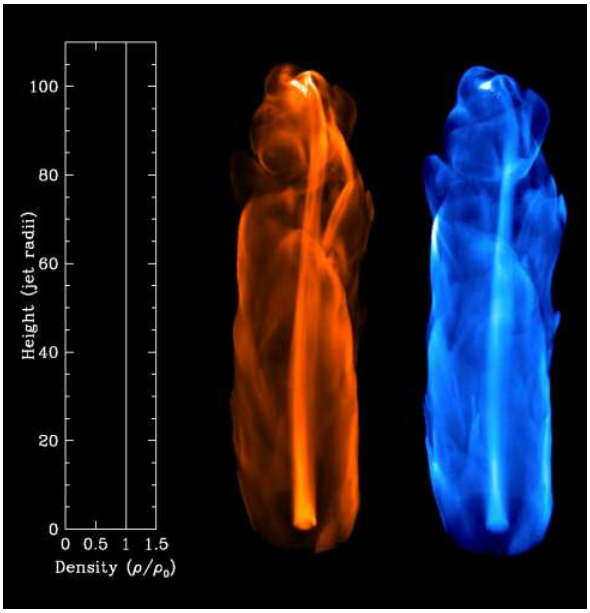

Fig. 1.— Synthetic 1.4 radio synchrotron (left) and 2 keV x-ray (right) observations of the HU jet, using identical contrast. Shown on the far left is the ambient density profile as a function of height from the x=0 plane.

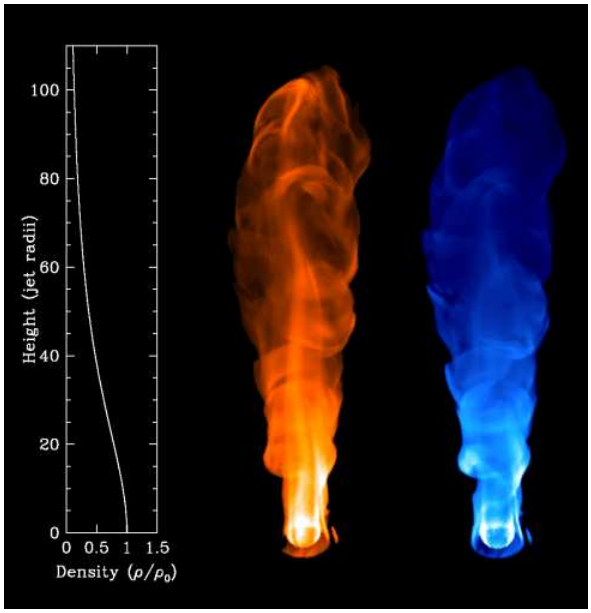

Fig. 2.— Synthetic 1.4 radio synchrotron (left) and 2 keV x-ray (right) observations of the LK jet, using identical contrast. Shown on the far left is the ambient density profile as a function of height from the x=0 plane.

III. RESULTS

(a) Synthetic Observations

Using the SYNTH ray tracing routine introduced in Tregillis et al (2002a, 2004) (detailed in Tregillis (2002b)), we construct radio synchrotron and CMB/inverse Compton x-ray synthetic observations from our simulated data. By combining the relativistic electron distributions and the vector magnetic field information, this routine constructs emissivities in each zone of our computational grid. These emissivities are then integrated along the line of sight to produce brightness maps for various emission mechanisms. The brightness maps are output in FITS format, which allows us to view them in standard astronomical analysis packages.

Figures 1 and 2 illustrate a sample set of synthetic observations constructed from our HU and LK runs, respectively. In each figure, the 1.4 GHz radio synchrotron and 2 keV x-ray brightness maps are shown next to the ambient density profile for that particular simulation. One obvious difference between the sets of observations is general morphology. We find that jets moving through a uniform medium tend to have a very pronounced backflow that forms a relatively wide cocoon, even near the $x = 0$ plane. The King-type atmospheres, on the other hand, tend not to form wide-based cocoons, since these backflows have to move against the ambient pressure gradient. This basic morphological distinction appears clearly in the sets of synthetic observations. Another interesting difference between the sets of observations is the presence or absence of terminal hotspots. The high-Mach jet in Figure 1 features clear regions of enhanced brightness near the end of both the radio and x-ray jets, while it is difficult to identify such features in the low-Mach brightness maps.

Additionally, we note that there is a much stronger correlation between the radio and x-ray maps in the case of the high-Mach run. Most of the features in Figure 1 can be identified in either map, while the radio and x-ray maps in Figure 2 do differ from one another. Specifically, it is very difficult to identify the jet in the LK jet x-ray brightness while there is a clearer contrast in the radio brightness. This difference presumably results from the fact that the CMB inverse Compton x-ray surface brightness is proportional to the electron column density at fixed energy, while the radio synchrotron surface brightness is constructed from both the electron column density and magnetic field information. We further note that both LK brightness maps in Figure 3 show a region of enhanced brightness near the base of the jet. This feature also appears in the HK brightness maps, and we attribute this increased electron column density to the stifled backflow in these two models.

(b) Energy Flow

By quantitatively following the flow of kinetic, thermal, magnetic and gravitational energy in each simulation and isolating contributions from jet plasma and the ICM using the "jet color" tracer, we can characterize how jet energetics are affected by the structure of the ambient medium and jet Mach number.

First, we can examine what fraction of the measured energy change takes place in the ambient material as compared to the jet. Figure 3 shows the fractional

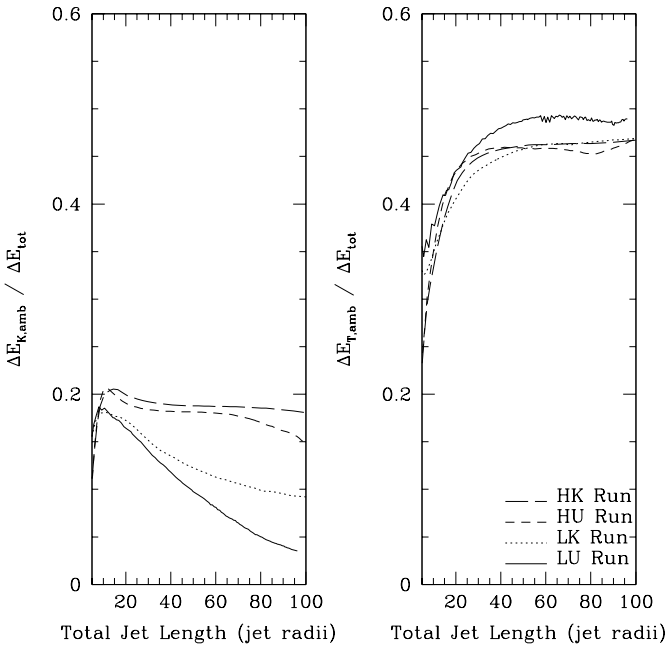

Fig. 3.— The ratio of the change in ambient kinetic energy (left) and ambient thermal energy (right) to the total inflowing jet energy. In all four runs, over half of the inflowing jet energy is transferred to the ambient medium, mostly in the form of thermal energy.

change in energy in the ambient medium, according to energy type, compared to the total change in energy on the grid. To first approximation, the total change in energy on the grid equals the inflowing jet energy, but some energy does exit from the open boundary surrounding the jet in the $x = 0$ plane. In our simulations, approximately 10% or less of the total jet energy leaves the grid in this manner, and our comparison run with a reflecting $x = 0$ boundary has illustrated that this loss does not affect the trends discussed here.

In each of the four runs, we see that at least half of the energy change on the grid is measured in the ambient medium, and most of this energy is in the form of ambient thermal energy. Furthermore, this trend is established well before the jets have reached full length, and the fraction of added thermal energy found in the ambient medium is nearly the same for each run. This is significant because it represents an efficient transfer of energy from the jet to the ambient medium in all of our models.

An interesting difference between runs of equal initial Mach number is the larger total change in energy for the uniform runs, as compared to the King-type runs. This is entirely a result of the longer jet propagation time in the uniform runs, and has the effect of raising the overall energy budget in the uniform runs, for a given jet length. By the time the jets have reached 90% of the grid length, the HU jet has advected onto the grid twice as much energy as the HK while the LU has advected 1.75 times as much energy as the LK. For both sets of Mach numbers, this difference is appreciable. Combined with our previous result, this means that a larger amount of energy enters the uniform environments than the King environments for a given Mach number since the fractional change in energy is comparable for all four runs.

IV. CONCLUSIONS

We have shown that the structure of the ambient medium can impact the morphology and energetics of simulated jets. Our synthetic radio and x-ray observations illustrate that jets moving into a uniform cluster environment develop more pronounced backflows than those moving into a stratified atmosphere. Additionally, synthetic observations of jets with higher Mach numbers feature more easily identifiable terminal hot spots and stronger radio/x-ray correlation than their low-Mach counterparts.

We find that energy transfer to the ambient medium is efficient for all of our simulations, with roughly half of the inflowing jet energy becoming thermal energy in the ambient medium during the course of jet propagation. Additionally, we note that jets introduce more energy onto the grid when moving through uniform environments than stratified atmospheres as a result of different jet propagation times. For a given Mach number and jet length, this has the effect of introducing more energy into uniform environments than King atmospheres.

ACKNOWLEDGEMENTS

This work is supported by the NSF grant AST03-07600 and by the University of Minnesota Supercomputing Institute. The work by DR was supported in part by KOSEF through grant R01-2004-000-10005-0. Also, we wish to thank Brian Cornell for his work in developing some of our visualization tools and Larry Rudnick for his input on our approach to synthetic observations.

REFERENCES

Blanton, E. L., Sarazin, C. L., & McNamara, B. R. 2003, ApJ, 585, 227

Böhringer H., Matsushita, K., Churazov, E., Ikebe, Y., & Chen, Y. 2002, A&A, 382, 804

Churazov, E., Sunyaev, R., Forman, W., & Böhringer, H. 2002, MNRAS, 332, 729

Dai, W., & Woodward P. R. 1998, ApJ, 494, 317

Harten, A. 1983, J. Comput. Phys., 49, 357

Jones, T. W., Ryu, D., & Engel, A. 1999, ApJ, 512, 105

King, I. 1962, AJ, 67, 8

Ryu, D., & Jones, T. W. 1995, ApJ, 442, 228

Ryu, D., Jones, T. W., & Frank, A. 1995, ApJ, 452, 785

Ryu, D., Miniati, F., Jones, T. W., & Frank, A. 1998, ApJ, 509, 244

Tregillis, I. L., Jones, T. W., & Ryu, D. 2001, ApJ, 557, 475

Tregillis, I. L., Jones, T. W., & Ryu, D. 2002a, in ASP Conf. Ser. 250, Particles and Fields in Radio Galaxies, ed. R. A. Laing & K. M. Blundell (San Francisco: ASP), 336

Tregillis, I. L. 2002b, PhD thesis, Univ. Minnesota

Tregillis, I. L., Jones, T. W., & Ryu, D. 2004, ApJ, 601, 778